

Figure-8 Storage Ring F8SR Non Neutral Plasma Confinement in Curvilinear Guiding Fields

Joschka F. Wagner

Institute of Applied Physics (IAP)
Workgroup Prof. Ulrich Ratzinger
Non Neutral Plasma-Group (NNP) Dr.Droba & Dr.Meusel
Goethe University Frankfurt
Germany

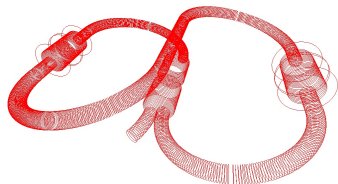
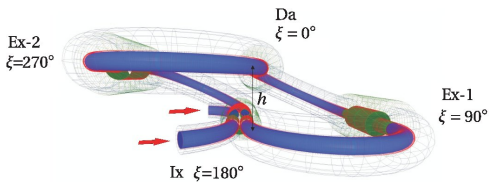
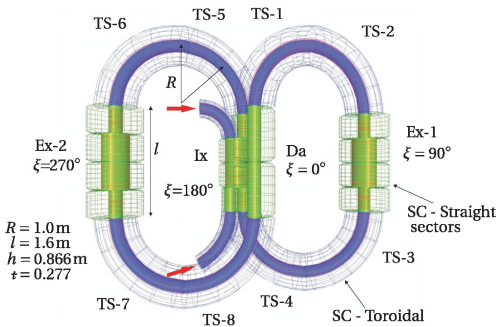
19.04.2013

Outline

- 1 Motivation
- 2 Traditional Storage Ring Concept
- 3 Magnetic Guiding Fields
- 4 Figure-8 Storage Ring
- 5 Numerical Magnetic Field Transformation, Analysis & Particle Simulation
- 6 Experiments at IAP
- 7 Outlook

Superconducting High Current Ion Storage Ring F8SR

- Magnetostatic $|\vec{B}| \approx 6$ T
- Beam Energy: $W = 150$ keV-1 MeV
- Beam Current: $I = 1$ -10 A
- Orbital revolution period: $T = 2 \mu\text{s}$
- Stored Beam Energy & Power:
 $E = 3$ J
 $P_{\text{max}} = 1.5$ MW

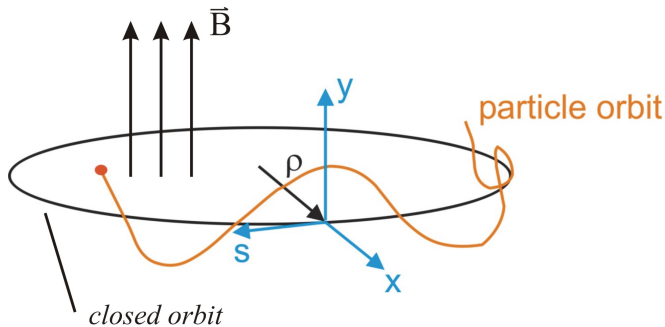


Why to build a new and such crooked Storage Ring - Motivation:

- astrophysical thin target experiments with well sharpened ΔE by electron cooling in a so called *Standard Mode*
- Fusion reactivity studies in a *High Current Mode* such as
 $p + {}^{11}\text{B} \rightarrow 3 {}^4\text{He} + 8.7 \text{ MeV}$
- multiple beam(species) experiments in *Collider Mode* down to center of mass collision energies of 100 eV
- space charge compensation by magnetic surface bounded secondary electrons
- multi ionisation of light atoms by an intense proton beam
- beam plasma interaction
- coulomb screening effects

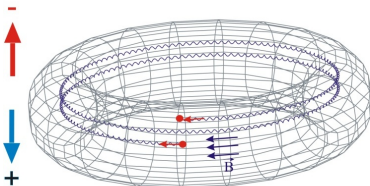
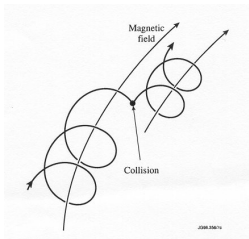
Traditional Storage Ring Concept

- achieving bending via dipole field
- **focussing** and corrections via quadrupoles & sextupoles
- closed orbit represents center of beam envelope



Magnetic Guiding Fields

- increasing the field strength up to $\approx 6\text{ T}$
→ fields become guiding fields
- field geometry can be chosen as toroidal.
problem: still drifts perpendicular to the torus plane



Magnetic Guiding Fields

- to achieve **focussing** use poloidal field components.
 → toroidal field gets a rotational transform t
 How? → bend the torus into a Figure-8
- off plane $\vec{R} \times \vec{B}$ drift vanishes in average due to changing direction of rotation

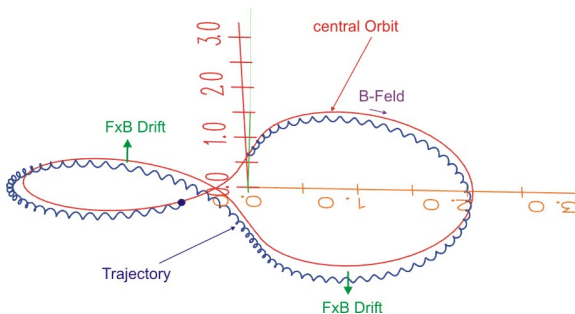
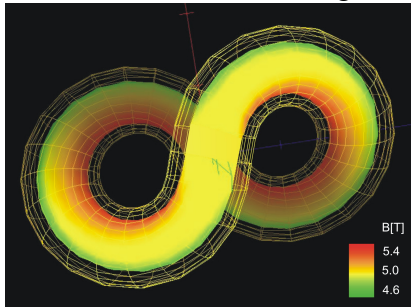


Figure-8 Storage Ring (**F8SR**)

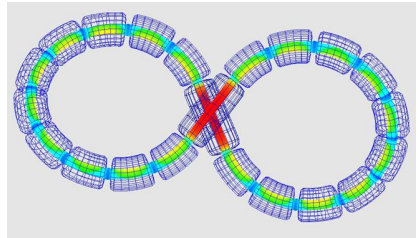
Studied Figure-8 Concepts

idealised mathematical design



- to see formation of magnetic surfaces
- first single particle dynamics

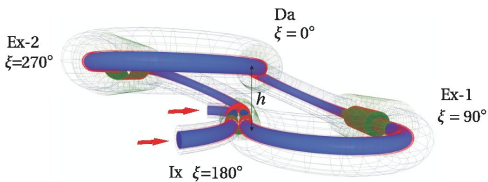
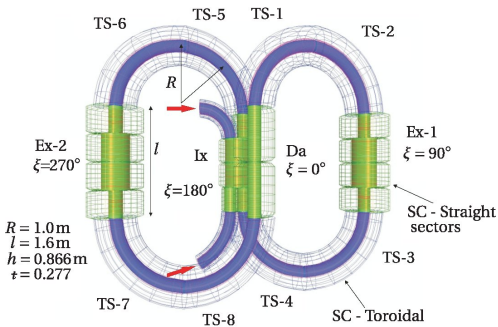
segmented design



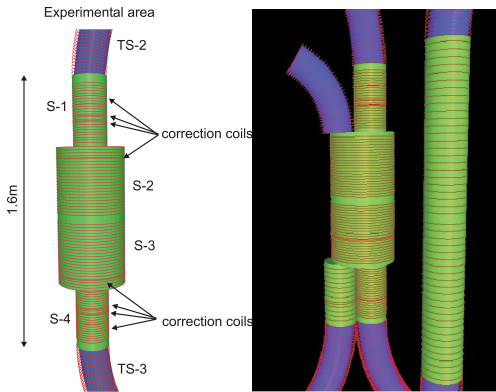
- first step for a concrete realisation
- lower costs, construction benefits
- problems with gaps and field discontinuities

Latest Figure-8 Design

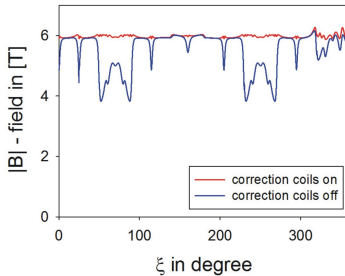
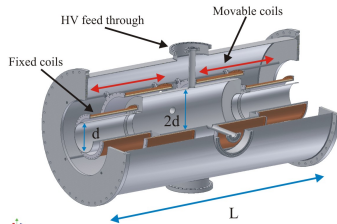
- realisation ideas of:
Injection-, Experimental- & Diagnosis area
- Magnetostatic $|\vec{B}| \approx 6 \text{ T}$
- Beam Energy: $W = 150 \text{ keV} - 1 \text{ MeV}$
- Beam Current: $I = 1 - 10 \text{ A}$
- Orbital revolution period: $T = 2 \mu\text{s}$
- Stored Beam Energy & Power:
 $E = 3 \text{ J}$
 $P_{\text{max}} = 1.5 \text{ MW}$



Latest Figure-8 Design



Preliminary designs



followed by field analysis and repetitive construction designs to optimise the compromise:
 beam transport ≠ experimenter liberties

Numerical Magnetic Field Transformation, Analysis & Particle Simulation

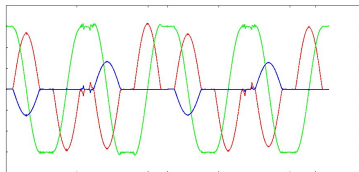
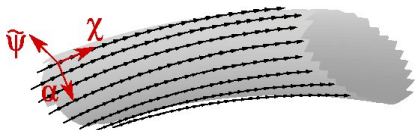
Simulation Method

- once the magnetic fluxdensity is high, a guiding center approximation can be done
- for stable long-term simulations the use of symplectic algorithms becomes clear (bounded error range)
- to switch in a symplectic form of canonical coordinates one needs to get magnetic fluxcoordinates (in particular: Boozercoordinates ψ, θ, ξ)
- in the end - combined with particle in cell (PIC) methods to establish simulations

Establishing Magnetic Fluxcoordinates

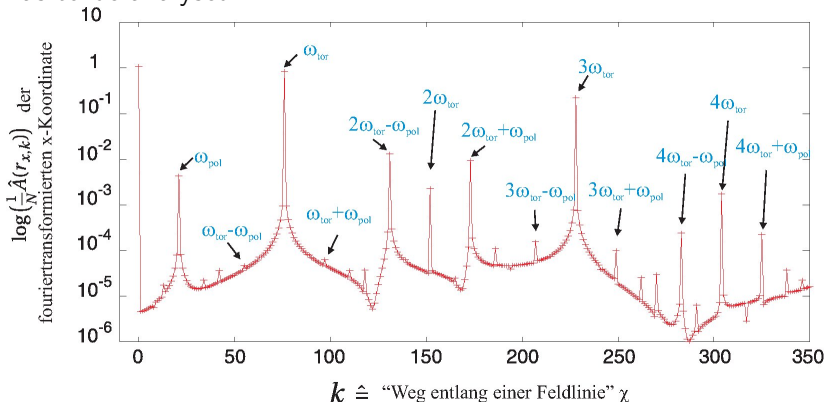
- conventional mapping: fieldline-tracing-method gives periodical functions :

$$\begin{array}{ccc}
 r_x(\chi) & r_y(\chi) & r_z(\chi) \\
 B_x(\chi) & B_y(\chi) & B_z(\chi) \\
 A_x(\chi) & A_y(\chi) & A_z(\chi)
 \end{array}$$



Establishing Magnetic Fluxcoordinates

1D-forward fouriertransformation gives frequency spectrum which has to be analysed



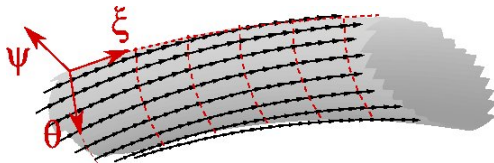
Establishing Magnetic Fluxcoordinates

- 2d-backward Fast-Fourier-Transformation and frequency splitting establishes curvilinear (non-orthogonal) magnetic fluxcoordinates (Boozercoordinates) propagating by 2π

$$\vec{r}(\psi, \theta, \xi) \quad \vec{B}(\psi, \theta, \xi) \quad \vec{A}(\psi, \theta, \xi)$$

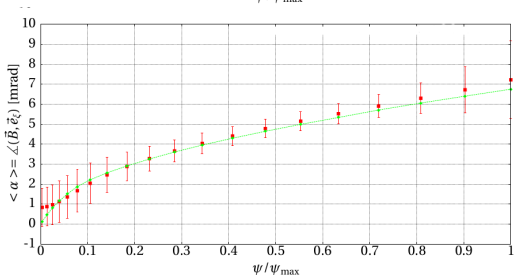
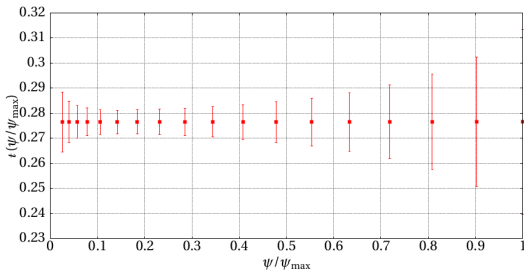
→ Co- and contravariant vector components

$$B_\psi, B^\psi, B_\theta, B^\theta, B_\xi, B^\xi$$



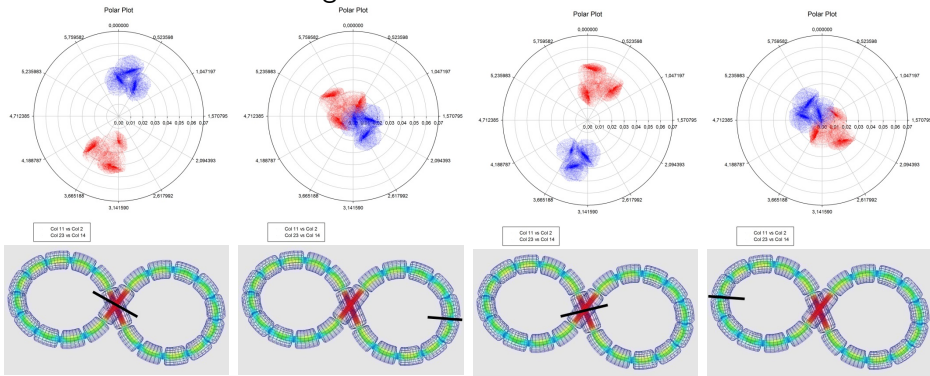
Numerical calculations vs. Theory

- coordinate transformation with 20 magnetic surfaces in total
- interesting parameters of boozercordinates were cross checked:
rotational transform $t = 0.277$
and for instance $\alpha = \angle(\vec{B}, \vec{e}_\xi)$



Beam Dynamics in F8SR

Co- and contratraveling ion beams



$$\xi = 0^\circ$$

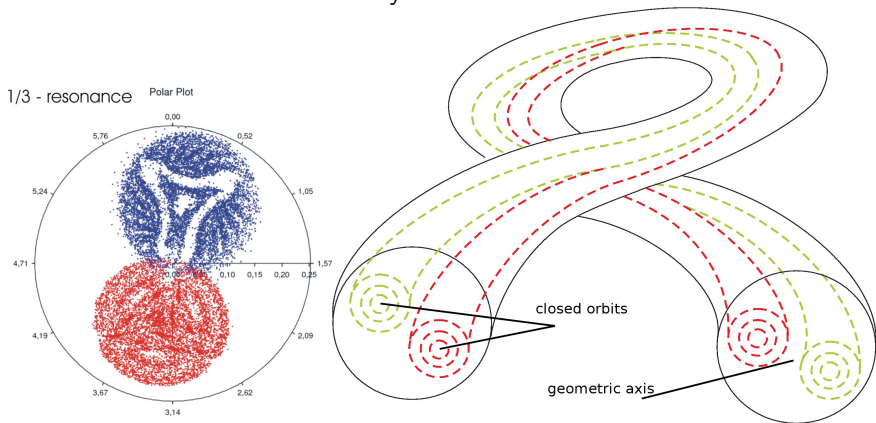
$$\xi = 90^\circ$$

$$\xi = 180^\circ$$

$$\xi = 270^\circ$$

Dynamics of Driftsurfaces via Symplectic Single Particle Simulation

closed orbits depends on: injection position, beam energy
→ orbits need to be evaluated by simulations

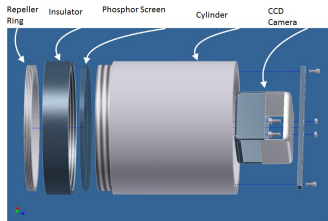


Experiments at Goethe University Institute of Applied Physics (IAP)



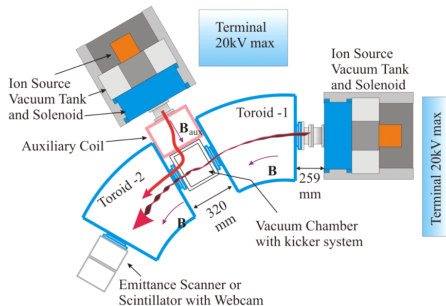
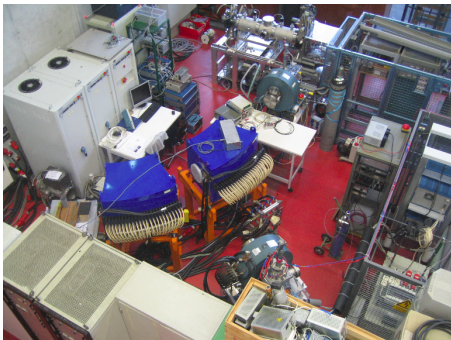


- emittance scanner: *transversal kick of beam in fringing field of toroid - position dependent*
- scintillator detector:
 - *mapping of beam motion in toroidal field*
 - *evidence of expected beam drift*
 - *detection of multi component beam focussing*
- transport through 2 toroids : *existing energy pass-band for optimum transition*



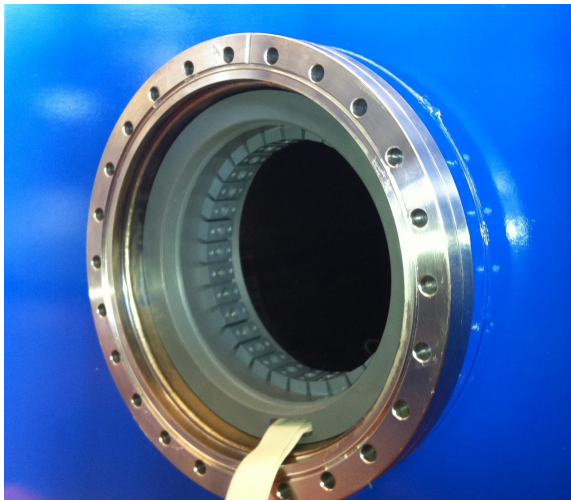
Exp. Setup for Toroidal Beam Transport & Injection Studies

- a second injector (ion-source + solenoid) was refurbished
- two faraday cups were build & installed for momentum filter studies in order to prepare single particle species injection [H.Niebuhr]
→ important for comparable closed orbit simulations



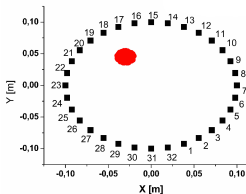
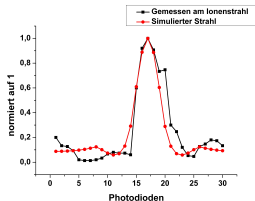
planned setup for injection experiments [N.Joshi]

Non-destructive Diagnostics via Residual Gas Monitor



Non-destructive Diagnostics via Residual Gas Monitor

Measured residual gas luminescence of H-ionspecies with simulation reconstruction



actual studies for online data acquisition between photodiodes and evaluationboard:

- 256 channels
- femtoampere currents
- integration times $160 \mu\text{s}$ -1 s



[Adem Ates]

Outlook

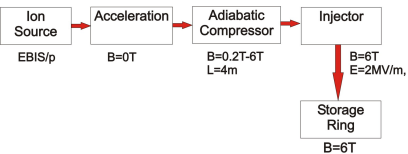
Adiabatic Compressor for Injection

- the facing problem is a smooth field transition

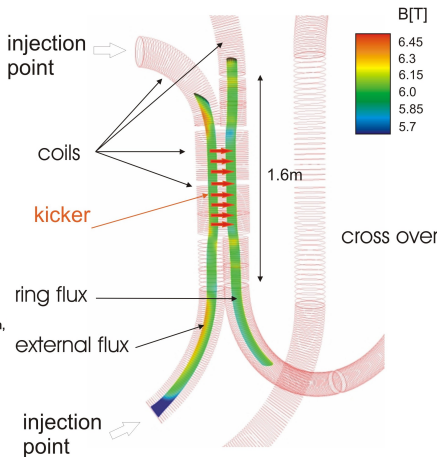
$$\mu = \frac{mv_{\perp}^2}{2B} \text{ must be constant}$$

$$\frac{dB}{dt} = \frac{\partial B}{\partial t} + v \frac{\partial B}{\partial x} < B \frac{\omega_c}{2\pi} =$$

$$\frac{qB^2}{2\pi m} \rightarrow v \frac{\Delta B}{\Delta z} < q \frac{B^2}{2\pi m}$$



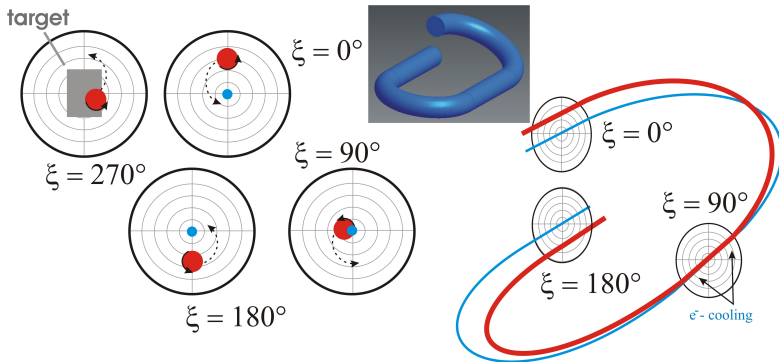
- repetitive coil(current) design with magnetic field analysis is needed



$$E \times B \text{ - kicker} \rightarrow \text{rep. rate } 4 \mu\text{s}, E = 2 \text{ MV/m}$$

Standard Mode with Electron Cooler

- e^- -gun ($E_{kin} \approx 120 \text{ eV}$) at geometric axis & e^- -collector 180° later
- due to high fields e^- are bound to the axis
- ion-beam drifts & rotates into e^- -beam simultaneously

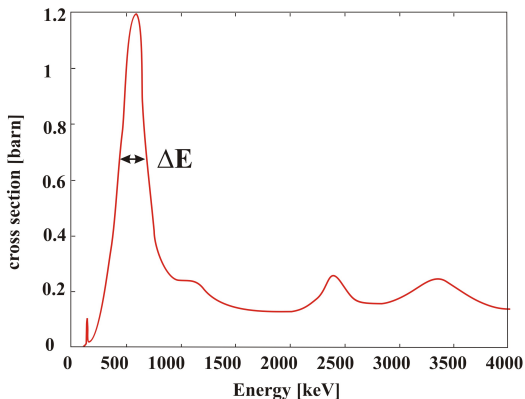


→ simulations are planned!

fusion Reactivity Studies in High Current Mode

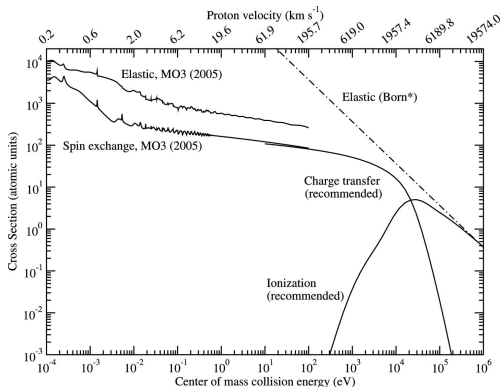
best fusion cross sections of $p + {}^{11}\text{B} \approx 500\text{-}600\text{ keV}$

→ a proton beam with a wider energy spread ΔE is fully acceptable (e^- -cooler off)



Low Energy Beam Beam Interactions in Collider Mode

Charge transfer problem: $H^+ + H \rightarrow H + H^+$

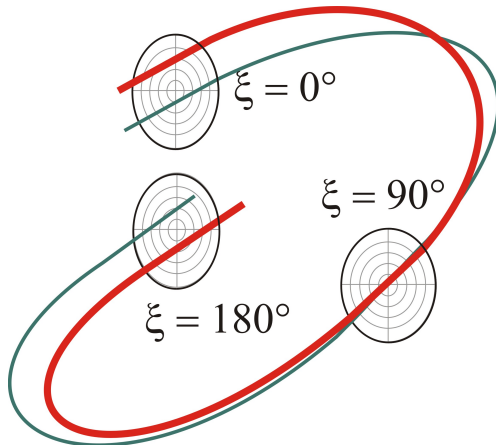


Low Energy Beam Beam Interactions in Collider Mode

→ injecting two beams ($E_{1,2} > 100 \text{ keV}$) with two axis-offsets and

$$v_1 - v_2 = \Delta v$$

→ leads to different closed orbits and collision energies $E_{\text{CMS}} < 100 \text{ keV}$



Thank you for your attention!

Institute of Applied Physics (IAP) Frankfurt
Prof. Ulrich Ratzinger

Non Neutral Plasma - Group
<http://nnp.physik.uni-frankfurt.de>

Contributors:

Dr. Martin Droba (field analysis, simulations, experiments)
[droba\(at\)iap.uni-frankfurt.de](mailto:droba(at)iap.uni-frankfurt.de)

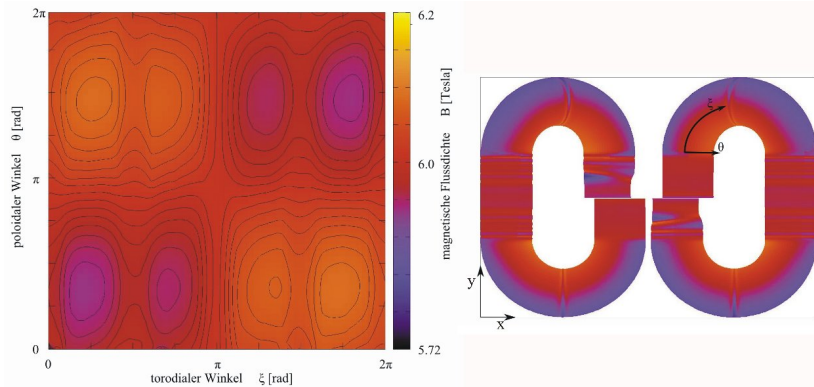
Dr. Oliver Meusel (experiments) *[O.Meusel\(at\)iap.uni-frankfurt.de](mailto:O.Meusel(at)iap.uni-frankfurt.de)*

Heiko Niebuhr (experiments) *[Niebuhr\(at\)stud.uni-frankfurt.de](mailto:Niebuhr(at)stud.uni-frankfurt.de)*

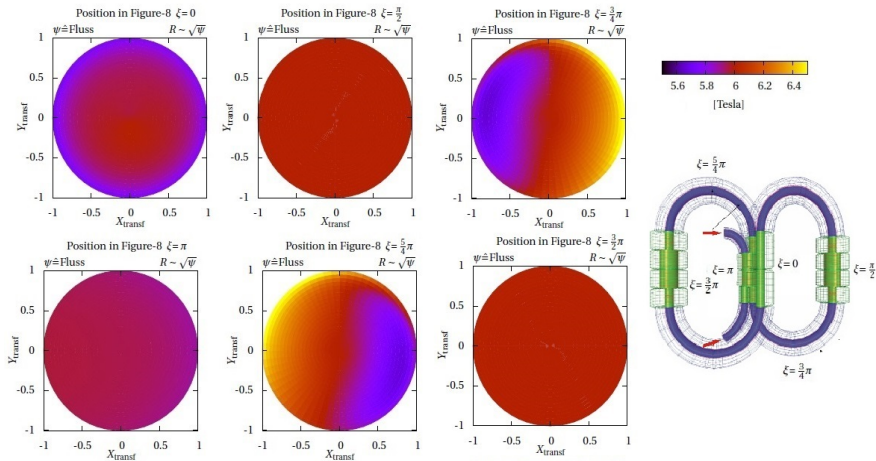
Adem Ates (diagnostics) *[aates\(at\)stud.uni-frankfurt.de](mailto:aates(at)stud.uni-frankfurt.de)*

Joschka F. Wagner (field analysis, simulations)
[j.f.wagner\(at\)stud.uni-frankfurt.de](mailto:j.f.wagner(at)stud.uni-frankfurt.de)

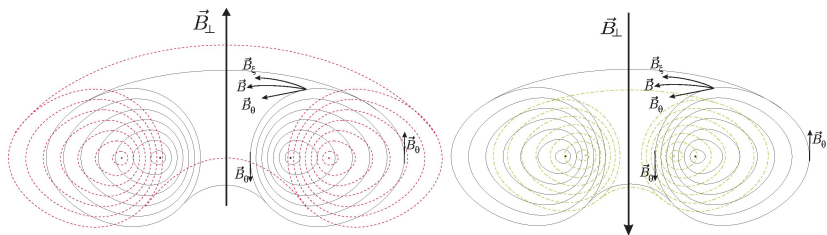
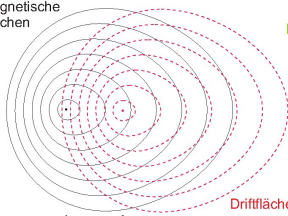
Map of Flux Density



Flux Density Profiles

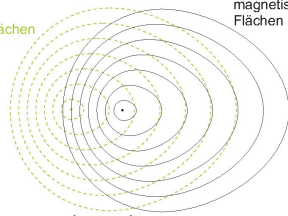


Driftsurfaces

magnetische
Flächenhorizontaler Shift Δ

Driftflächen

Driftflächen

horizontaler Shift Δ magnetische
Flächen

$$\Delta = \mp \frac{2\pi\beta r_L}{l}$$

Drift Hamiltonian & Canonical Variables

$$P_\theta = \frac{q\psi}{2\pi} \qquad P_\xi = \frac{\mu_0 G}{2\pi|B|} m v_{||} - t \frac{q\psi}{2\pi}$$

$$g = \frac{\mu_0 G}{2\pi}$$

$$H = \frac{1}{2m} \frac{(P_\xi + t P_\theta)^2 (2\pi)^2 |B|^2}{\mu_0^2 G^2 m^2} + \mu |B| + q\Phi$$